Available online at www.sciencedirect.com

SciVerse ScienceDirect

Ceramics International 39 (2013) 6611–6618

CERAMICS INTERNATIONAL

www.elsevier.com/locate/ceramint

Electrochemical study of NiO nanoparticles electrode for application in rechargeable lithium-ion batteries

Alok Kumar Rai, Ly Tuan Anh, Chan-Jin Park, Jaekook Kim*

Department of Materials Science and Engineering, Chonnam National University, 300 Yongbong-dong, Bukgu, Gwangju 500-757, South Korea

Received 3 January 2013; received in revised form 8 January 2013; accepted 28 January 2013
Available online 4 February 2013

Abstract

Nickel oxide nanoparticles were synthesized via a simple and inexpensive microwave-assisted synthesis method within a fast reaction time of less than 20 min. The calcination of as-prepared precursor at 600 °C produces single phase nickel oxide. The lattice structure and morphology of the sample were investigated by X-ray diffraction, field-emission scanning electron microscopy and field-emission transmission electron microscopy. The particle size range of the nickel oxide nanoparticles varied from 50 to 60 nm. Nickel oxide nanoparticles exhibited good electrochemical performances as an anode material for lithium-ion batteries. The prepared nickel oxide anode revealed a large initial discharge capacity of 1111.08 mAh g^{-1} at 0.03 C rate and retained 80% of initial capacity (884.30 mAh g^{-1}) after 20 cycles. Furthermore, at elevated rate of 3.7 C, the charge capacity of the nickel oxide electrode was as high as 253.1 mAh g^{-1}, which was 35% greater than that of commercial bulk nickel oxide (188 mAh g^{-1}). The enhancement of the electrochemical performance was attributed to the high specific surface area, good electric contact among the particles and easier lithium ion diffusion.

Keywords: A. Microwave processing; D. Transition metal oxides; E. Batteries

1. Introduction:

Rechargeable lithium-ion batteries have been the most widely used batteries in portable electronic device market for the past few years. Carbon-based materials, such as graphite, have been employed as anodes in commercial available lithium-ion batteries since 1991, due to their high deliverable operation potential, good electronic conductivity, high Li^+ chemical diffusion coefficient and low volume changes during Li^+ intercalation/de-intercalation [1]. However, their limited capacities (the theoretical capacity of graphite is 372 mAh g^{-1}) appear to be an obstacle to satisfy the urgent need for rechargeable lithium-ion batteries with high energy and power densities for hybrid and plug-in hybrid electric vehicles [2,3]. On the other hand, various carbon nanostructures, such as porous carbon, which can provide fast kinetics and are structurally stable during charge/discharge are still under intensive development [4].

Recently, transition metal oxides (MO, where M is Ni, Co, Cu or Fe) have attracted much attention and widespread interest in the energy industry, due to their numerous desirable properties, such as their high theoretical capacity (500–1000 mAh g^{-1} compared with conventional graphite) on the basis of their unique conversion mechanism, long cycle life and high recharging rates [5–8]. These impressive properties make them promising candidates to use as anode materials in lithium-ion batteries. Nevertheless, anodes based on pure transition metal oxides suffer from poor cycling performance, owing to the tendency of particle agglomeration during lithium-ion insertion/extraction processes and mechanical instabilities caused by drastic volume changes, which ultimately result in increased diffusion lengths and electrical disconnection from the current collector [9,10]. So, in recent years, much research has been focused on improving their electrochemical performance, and many methods have been proposed in this regard. For example, forming composites

*Corresponding author. Tel.: +82 62 530 1703; fax: +82 62 530 1699.
E-mail address: jaekook@chonnam.ac.kr (J. Kim).

0272-8842/$ - see front matter © 2013 Elsevier Ltd and Techna Group S.r.l. All rights reserved.
http://dx.doi.org/10.1016/j.ceramint.2013.01.097

with conductive materials such as carbon is a very common and useful method, but often reduces the mass specific capacity [11,12]. So, preparing materials with a special morphologies such as a porous structure [13–16], nanoarrays [6,17], microspheres [18–22] and some others [23] to enhance the electrochemical performance has attracted much attraction.

Owing to its superior properties such as its high theoretical capacity (718 mAh g^{-1}), higher density (6.81 g cm^{-3}) than that of graphite (2.268 g cm^{-3}), nontoxicity and low material cost, nickel oxide (NiO) has been under extensive investigation as an important functional inorganic material, for use in fuel cells [24], solar cells [25,26], lithium-ion batteries (LIBs) and supercapacitors [27–30]. In the past few decades, many methods have been reported for the synthesis of NiO particles with various morphologies, such as nanoplates, nanorods, nanowires, nanotubes, and 3D-rose like and hollow microspheres particles [6,31–50], but achieving better long term and high rate performances, required to make them a qualified anode material for high power lithium-ion batteries, is still problematic. Therefore, strategy to develop NiO electrode materials with intrinsically high-rate capability remains significant. Recently, microwave heating has been used as a new rapid synthesis route for preparing metallic or bimetallic nanoparticles [51]. One obvious merit of microwave-assisted process is the marked decrease in reaction time to less than 20 min, which is significantly less than the reaction time needed in traditional or sol–gel methods. In microwave heating the energy is directly transferred to the material through molecular interaction and, therefore, it has several beneficial effects, including rapid volumetric heating, shorter reaction times, selective heating, and an additional driving force for diffusion mechanism compared to conventional thermal processing. In light of the above discussion, the present study reports the synthesis of NiO nanoparticles via a simple and inexpensive microwave-assisted synthesis method, followed by calcination at 600 °C in air atmosphere. A series of characterization procedures indicated that there was an enhancement of the electrochemical performance of the NiO nanoparticles, which is attributed to the short diffusion length and large surface-to-volume ratio that allows for a large electrode/electrolyte contact area. In addition, we have also checked the ex-situ DSC measurements and found a higher thermal stability in comparison to other anodes.

2. Experimental

2.1. Materials synthesis

Analytical grade nickel (II) acetate ($Ni(CH_3COO)_2 \cdot 4H_2O$) (98%, Aldrich) was used as a precursor. In a typical synthesis, 0.01 mol of nickel acetate were dissolved in 50 ml of deionized water (DI) with magnetic stirring at room temperature to form a homogeneous solution. Ammonia solution (10 ml, Daejung 25%) was added to the above solution and subsequently stirred for 3 h. The resulting mixture was transferred to a conventional microwave oven (MM–M 301, LG-Korea), with the specification of 1000 W at 2450 MHz, and was heated around 140–150 °C for 10 min by microwave irradiation. After the reaction, the mixture was cooled to room temperature. The resultant as-prepared dried mixtures were ground to fine powders before heating at 600 °C for 3 h in air atmosphere.

2.2. Material characterization:

The X-ray diffraction (XRD) pattern was obtained by a Shimadzu X-ray diffractometer with Cu Kα radiation ($\lambda = 1.5406$ Å). The morphology of the final product was characterized by field-emission scanning electron microscopy (FE-SEM, S-4700 Hitachi). Field-emission transmission electron microscopy (FE-TEM) and high-resolution transmission electron microscopy (HR-TEM) images with the corresponding selected-area electron diffraction (SAED) patterns were obtained by a FEI Tecnai F20 with an accelerating voltage of 200 kV. For the FE-TEM images, powder samples were ultrasonically dispersed in ethanol and a few drops were coated on copper grids and the solvent was subsequently allowed to evaporate in air at room temperature.

2.3. Electrochemical measurements

Electrochemical experiments were carried out using 2032 coin-type cells assembled in an argon-filled glovebox. For the working electrode fabrication, a slurry was prepared by mixing the active material (NiO nanoparticles) with super-P and poly vinylidene difluoride at a weight ratio of 80:10:10 in N-methyl-2-pyrrolidone. The resultant slurry was uniformly pasted on Cu-foil with a blade, dried at 120 °C in a vacuum oven and pressed between stainless steel twin rollers. Afterward, the foil was punched into circular discs and pressed, and coin cells were assembled with lithium metal as the counter electrode and a Celgard 2400 membrane together with glass fiber as a separator. The cells were kept in a glovebox for 12 h before electrochemical measurements. The electrolyte used was 1 M $LiPF_6$ dissolved in a mixture of ethylene carbonate (EC) and dimethylcarbonate (DMC) (1:1 in volume ratio). The discharge-charge measurements (wonatech WBCS 3000) were performed over the potential range of 0.005–3.0 V vs. Li^+/Li at different current densities. Cyclic voltammetric (CV) measurement of the electrode was performed on an AUTOLAB potentiostat (PGSTAT302N) with a scan rate of 0.1 mV s^{-1} between 0 and 3 V (vs. Li^+/Li). Electrochemical impedance spectroscopy (EIS) measurements of the electrode were also carried out on an AUTOLAB potentiostat (PGSTAT302N). Before the measurements, the electrode was cycled for 3 cycles and then measured in the frequency range from 0.01 Hz to 1.0 MHz. A small ac signal of 5 mV in amplitude was used as the perturbation

of the system throughout the tests. EIS was used to measure the electronic conductivities of the assembled cell using lithium foil acting as both the counter and reference electrodes. In order to investigate the thermal safety of the prepared NiO sample, ex-situ differential scanning calorimeter (DSC) measurement was performed on this sample up to 400 °C at a heating rate of 5 °C/min in a nitrogen atmosphere using a Q1000 (TA instruments, USA) at the Korea Electrotechnology Research Institute (KERI). First the NiO electrode was discharged and maintained at 0.005 V for 12 h during the 1st discharge cycle. After the electrochemical reaction, the electrode was rinsed with DMC in order to remove the remaining electrolyte and then dried in an Ar-filled glovebox at ambient temperature. The electrode was then separated from the stainless steel mesh current collectors and sealed via a micro-tube in an Ar-filled glovebox to avoid exposure to air.

3. Results and discussion

3.1. Crystal structure and morphology

XRD measurement was employed to investigate the phase and structure of the synthesized sample. Fig. 1 shows the XRD pattern of the prepared NiO nanoparticles powder. All the diffraction peaks at 37.29°, 43.30°, 62.96°, 75.43° and 79.36° [(111), (200), (220), (311) and (222) reflections, respectively] are in good agreement with the standard crystallographic data (JCPDS-No 04-0835, space group *Fm3m*), indicating nanocrystalline cubic structure of the sample. In addition, XRD pattern also shows that the nickel precursor has been fully transformed into crystalline NiO.

The morphology of the prepared NiO nanoparticles was studied by FE-SEM and the recorded image is displayed in Fig. 2(a). The photograph clearly shows irregularly-shaped particles with particle sizes of about 50–60 nm. In addition, particle agglomeration is also visible. To further understand the morphology and structural characteristics of the NiO nanoparticles, FE-TEM was also employed. Fig. 2(b) presents a typical TEM image, which confirmed the overall morphology of the as-prepared product. The agglomeration of the NiO nanoparticles with an irregular shaped morphology was observed. The FE-TEM picture shown in Fig. 2(c) provides information on the size and morphology of the NiO nanoparticles and their state of agglomeration. A few of the smaller nanoparticles aggregate into secondary particles, probably due to their extremely small dimensions and high surface energies. The inset of Fig. 2(c) represents the HR-TEM image of the sample which reveals unidirectional fringe patterns and thereby indicates the high crystalline nature of the sample. The interplanar spacing '*d*' (distance between 2 successive lines) measured from the fringe pattern is 2.08 Å, which corresponds to the (200) plane, as observed from the XRD results in Fig. 1. Fig. 2(d) shows that the corresponding SAED originating from the NiO nanoparticles which demonstrated clear rings with superimposed bright spots that are indicative of the nanocrystalline nature of NiO nanoparticles. Grain size is small, so sub-grains within bigger grains are also present within the selected area aperture. These grains give extra spots. The SAED pattern could be indexed on the basis of the *Fm3m* space group and the calculated planes (the obtained *d*-values corresponding to the spots/rings) are matched very well with those of the XRD pattern.

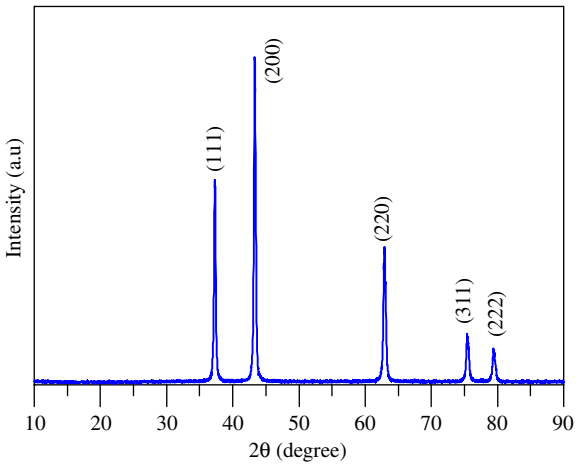

Fig. 1. XRD pattern of NiO nanoparticles synthesized at 600 °C for 3 h in air.

3.2. Electrochemical performance:

Fig. 3(a) shows the voltage profiles for the NiO nanoparticle anode in the range 0.005–3.0 V at a rate of 0.03 C for the 1st, 2nd, 5th and 10th cycles. The cells show an irreversible discharge capacity loss during the first cycle and the values stabilized on subsequent cycling. During the first discharge, the initial discharge capacity for NiO nanoparticles is 1111.08 mAh g^{-1}. At the same time, the voltage decreases steeply to 0.6 V where a plateau region sets in and continues until the discharge capacity of 840.1 mAh g^{-1}, which corresponds to a consumption of 2.34 mol of Li per mole of NiO. Another slope observed at 0.55 V, with a total initial discharge capacity of 1111.08 mAh g^{-1}, is associated with a consumption of 3.09 mol of Li per mole of NiO. According to the mechanism ($NiO+2Li^{+}+2e^{-} \Leftrightarrow Li_2O+Ni$), the discharge process should consume 2.0 lithium per NiO, but the experimental value is 3.09 lithium per NiO nanoparticles. The capacity of the initial discharge process may be attributed to both the formation of a solid electrolyte interface (SEI) film and a polymeric gel-type layer on the surface of the material, resulting from the solvent decomposition of the electrolyte [52,53]. The first charge profile of the NiO nanoparticles shows a strong polarization of ~1.3 V followed by a voltage plateau at ~2.2 V. The peak at 2.2 V during the charge cycle corresponds to the reverse reaction of formation of NiO from Ni and Li_2O. The first charge capacity (Li^{+} deinsertion) is 780.5 mAh g^{-1} (2.17 mol of Li) [6]. The irreversible capacity loss during the first discharge/charge cycle is ~331 mAh g^{-1}.

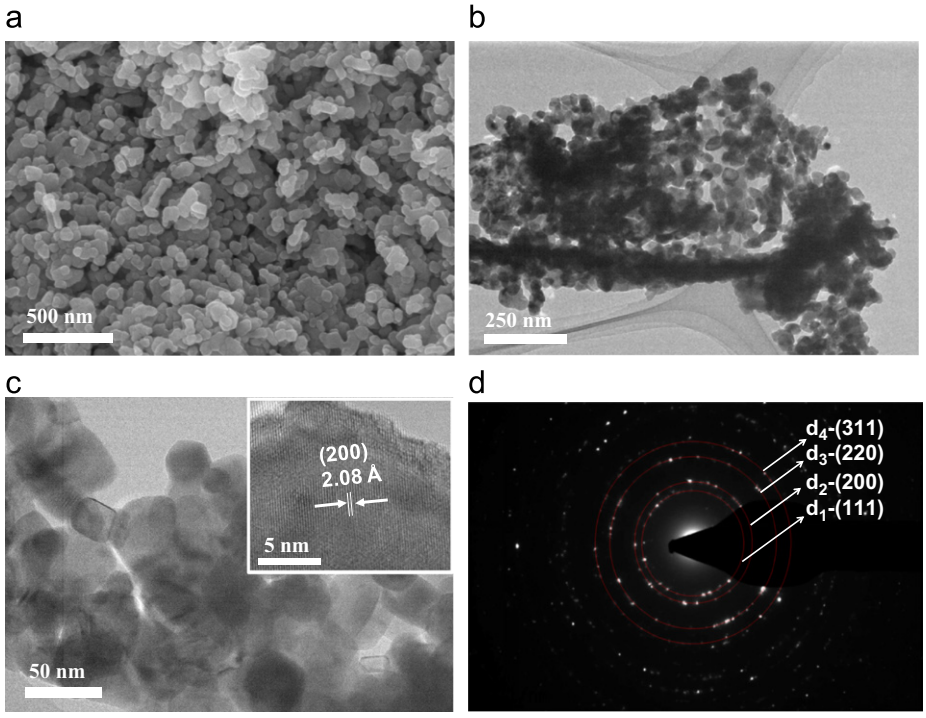

Fig. 2. (a) FE-SEM micrograph of NiO nanoparticles, (b) Low-magnification FE-TEM, (c) high-magnification FE-TEM images, and (d) corresponding SAED pattern of NiO nanoparticles. The inset in (c) is the HR-TEM image of NiO nanoparticles with [200] plane.

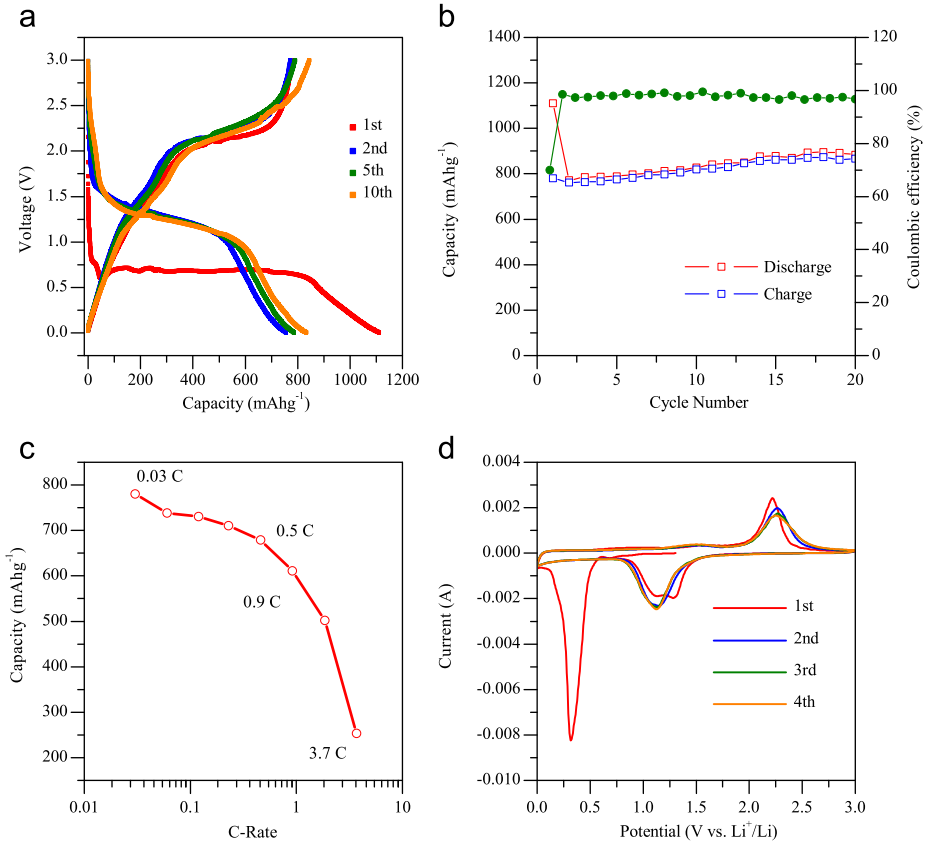

Fig. 3. Electrochemical performance of the NiO nanoparticles electrode. (a) Discharge/charge voltage profiles at the rate of 0.03 C. (b) Capacity retention and coulombic efficiency plots between 0.005–3.0 V at the rate of 0.03 C. (c) The charge capacity as a function of C-rate is plotted. (d) Cyclic voltammograms at a scan rate of 0.1 mV s^{-1}.

Generally, the irreversible capacity loss during the first cycle can be attributed to the incomplete decomposition of SEI film and Li_2O. The other factors, such as the intrinsic nature of the material with specific morphology are also apparent [22]. A reversible discharge capacity of 755.4 mAh g^{-1} was achieved in the second cycle, which gradually increases to about 785.4 and 832.9 mAh g^{-1} after the 5th and 10th cycles, respectively, whereas the coulombic efficiency reached more than 75%. The increase in specific capacities during consecutive cycles is a common feature observed for nanocrystalline electrodes and is attributed to the enhanced probabilities of finding more favorable Li-ion migration pathways in the nano-scaled NiO particles.

Fig. 3(b) shows the discharge/charge capacity profile vs. cycle number of the NiO nanoparticles electrode at a rate of 0.03 C. As can be observed, a discharge capacity of 884.30 mAh g^{-1}, which is equivalent to 80% of the initial capacity, is registered after 20 cycles with 98% of coulombic efficiency. There can be a possible reason for the better cycling performance of the nanocrystalline NiO electrode such as the annealed NiO nanoparticles have a high degree of crystallization, resulting in the reduction in the number of lattice defects, which facilitates the lithium ions insertion and extraction processes. It can be clearly observed that microwave-assisted synthesized NiO nanoparticle electrode provides impressive performance and unique behavior with increasing values of the discharge/charge capacity and cycle number. Additionally, the observed discharge/charge capacity and cycle number values are not much lower than those reported for NiO nanoparticles, but the synthesis strategy adopted in the present study is cost-effective and simple compared to that in the previously reported counterparts [20,54–56].

Moreover, NiO nanoparticles electrode shows good C-rate behavior ranging from 0.03 C to 3.7 C, as shown in Fig. 3(c). The cell was first cycled at a low current rate of 0.03 C, where a stable specific charge capacity of about 780.5 mAh g^{-1} was obtained. The charge capacity was as high as 738.5, 730.3, 710.7, 678.7, 611.4 and 501.9 mAh g^{-1} after the current rate was increased to 0.06 C, 0.1 C, 0.2 C, 0.5 C, 0.9 C and 1.6 C, respectively, which are still higher than the theoretical capacity of graphite (372 mAh g^{-1}). Even at a high current rate of 3.7 C, more than 32% of the capacity (253.1 mAh g^{-1}) is retained.

The CV curves of the NiO nanoparticle electrode were tested over the voltage range from 0.0 to 3.0 V (vs. Li^+/Li) at a scan rate of 0.1 mV s^{-1}. As shown in Fig. 3(d), there was a characteristic cathodic peak at around 0.32 V in the first cycle, which corresponds to the initial reduction of NiO to metallic Ni nanoparticles and the formation of a partly reversible SEI layer [6]. Two anodic peaks were also observed at around ~2.24 and 1.52 V, which correspond to the decomposition of Li_2O and the electrolyte, respectively. This agrees well with the previously reported characteristics of NiO nanoparticle anode materials [20,57]. These peaks shift to about 1.13 and 2.24 V, respectively, in the subsequent cycles, due to the drastic lithium driven structural or textural modifications [52,57].

The increased electronic conductivity of the NiO nanoparticle anode is clearly demonstrated by EIS. Fig. 4(a) shows the EIS spectrum of the NiO nanoparticle electrode. Before the measurement, the electrode was cycled for 3 discharge/charge cycles and kept until a stable open-circuit voltage is reached. Fig. 4(b) shows the zoomed part of Fig. 4(a) in the high frequency region and the plotted data was fitted using the Non-Linear Square Fit method and the corresponding equivalent circuit is also shown in Fig. 4(b). The parameters, R_s, R_{sf}, R_{ct} and W in the circuit correspond to the ohmic resistances of the electrolyte, SEI and Li-ion charge transfer and the Warburg impedance, respectively. Generally, the high frequency semicircle and the semicircle in the medium-frequency region are attributed to the SEI film and/or contact resistance and the Li^+ charge-transfer impedance at the electrode/electrolyte interface, respectively [58,59]. The inclined line observed in the low frequency range at an angle of approximately 45° to the real axis corresponds to the lithium-diffusion

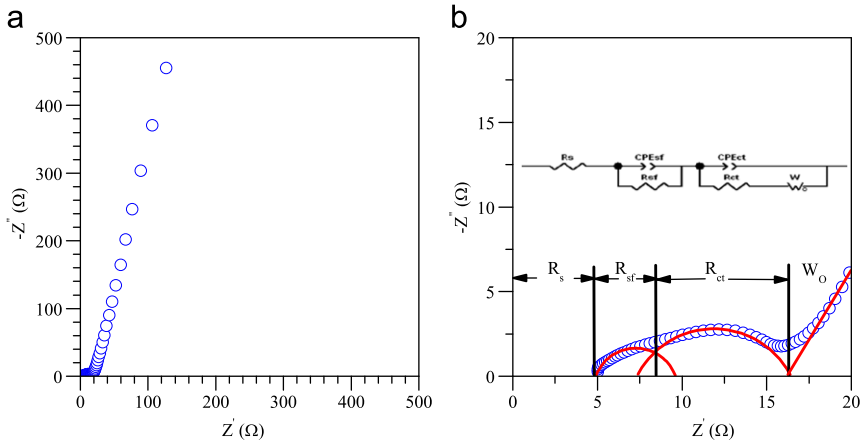

Fig. 4. (a) EIS spectrum of NiO nanoparticles electrode in the frequency range between 0.01 Hz and 1.0 MHz at room temperature and (b) high frequency zoomed part of EIS spectrum with equivalent circuit.

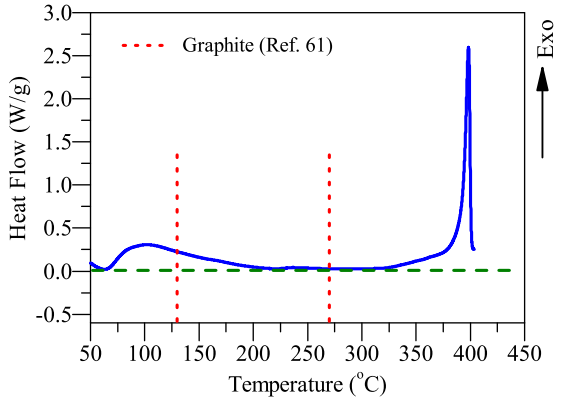

Fig. 5. DSC curve of the fully lithiated NiO nanoparticles electrode.

processes within the electrode and is known as the Warburg impedance [60]. In the present case, the impedance spectra at high frequencies are fitted by two merging semicircles, such as the smaller one corresponding to the higher frequency domain which in turn corresponds to the SEI film resistance and the bigger semicircle at the apparently lower or intermediate frequencies corresponds to the charge-transfer resistance. The results of the fitting analysis indicate that the SEI film and charge-transfer resistances are 3.6 Ω and 7.9 Ω respectively. Precisely, the value obtained for the latter one is much less, which is most probably due to the facile charge transfer at the nano-scale NiO walls/electrolyte interface and large reduction in the charge-transfer impedance. This reduction of the charge transfer resistance is beneficial to enhance the electron kinetics in the electrode material and, hence, improve the electrochemical performance of the NiO nanoparticle electrode for lithium storage.

Materials safety is also a major consideration for batteries in automotive applications. We performed ex-situ DSC measurements on the NiO anode material up to 400 °C to determine at what temperatures thermal events would occur and how much energy would be released. Fig. 5 shows the ex-situ DSC profile of the NiO nanoparticle anode material obtained after first discharge cycle. This microwave-assisted synthesized NiO anode material revealed significant differences in its thermal characteristics in comparison to the other well-known, commercially used anode material such as graphite [61]. It can be clearly observed from Fig. 5 that the ex-situ DSC profile of NiO indicates a widely stable thermal window, as observed from the absence of exothermic peaks up to the 400 °C. The authors believe that the exothermic peak at 400 °C is caused by the thermal decomposition of the products of the reaction, whereas graphite possesses exothermic DSC peaks around ~130 °C and in the range of ~270–300 °C, which are indicated by the marked lines in Fig. 5. Further, the total energy released by graphite is much greater than that released by NiO [61]. Thus, it is reasonable to conclude that graphite exhibits an apparently lower thermal stability domain in comparsion to that of NiO. Moreover, literature reports of a DSC exothermic peak in another well-known anode material $Li_4Ti_5O_{12}$ at ~300 °C [62]. Hence, it can be reasonably argued that NiO possesses potential advantages that warrant its consideration as an alternative anode to commercially used anodes.

4. Conclusions

In this study, pure NiO nanoparticles were successfully synthesized by a simple and fast microwave-assisted synthesis with a reaction time of less than 20 min, followed by calcination at 600 °C for 3 h. The synthesized NiO nanoparticles were characterized using XRD, FE-SEM and FE-TEM techniques. The FE-SEM and FE-TEM images show that the NiO nanoparticles have sizes of about 50–60 nm with an irregular shaped morphology. The NiO nanoparticles electrode shows good rate capability and high capacity when used as an anode in lithium-ion batteries. The NiO electrode delivers an initial discharge capacity of 1111.08 mAh g^{-1} at 0.03 C and, more importantly, can retain 80% of initial capacity (884.30 mAh g^{-1}) after 20 cycles. Moreover, the NiO electrodes maintain a charge capacity of 253.1 mAh g^{-1} even at a rate as high as 3.7 C, which is 35% higher than that in commercial or bulk NiO electrode (only 188 mAh g^{-1}). The enhanced electrochemical characteristics of the NiO nanoparticle electrodes arise from their relatively high specific surface area, good electric contact among the particles and easier lithium ion diffusion. The ex-situ DSC measurements performed on the prepared NiO sample indicated that it possessed higher thermal stability compared to other anodes, making it attractive for alternative and safer anodes. Moreover, the simple preparation method enables the possibility of their easier production on a large scale.

Acknowledgments

This research was supported by WCU (World Class University) program through the Korea Science and Engineering Foundation funded by the Ministry of Education, Science and Technology (R32-20074). This research was financially also supported by the Ministry of Education, Science Technology (MEST) and National Research Foundation of Korea (NRF) through the Basic Research Laboratories (BRL) Program (2011-0001567) and the Human Resource Training Project for Regional Innovation.

References

[1] M. Endo, C. Kin, K. Nishimura, T. Fujino, K. Miyashita, Recent development of carbon materials for Li ion batteries, Carbon 38 (2000) 183–197.
[2] M. Winter, J.O. Besenhard, M.E. Spahr, P. Novak, Insertion electrode materials for rechargeable lithium batteries, Advanced Materials 10 (1998) 725–763.
[3] W.V. Schalkwijk, B. Scrosati, Advances in Lithium-Ion Batteries, Kluwer Academic/Plenum Publishers, New York, 2002.

[4] N.A. Kaskhedikar, J. Maier, Lithium storage in carbon nanostructures, Advanced Materials 21 (2009) 2664–2680.
[5] P.L. Taberna, S. Mitra, P. Poizot, P. Simon, J.M. Tarascon, High rate capabilities Fe_3O_4-based Cu nano-architectured electrodes for lithium-ion battery applications, Nature Materials 5 (2006) 567–573.
[6] B. Varghese, M.V. Reddy, Z. Yanwu, C.S. Lit, T.C. Hoong, G.V. Subba Rao, B.V.R. Chowdari, A.T.S. Wee, C.T. Lim, C.H. Sow, Fabrication of NiO nanowall electrodes for high performance lithium ion battery, Chemistry of Materials 20 (2008) 3360–3367.
[7] G.X. Wang, Y. Chen, K. Konstantinov, M. Lindsay, H.K. Liu, S.X. Dou, Investigation of cobalt oxides as anode materials for Li-ion batteries, Journal of Power Sources 109 (2002) 142–147.
[8] S.L. Chou, J.Z. Wang, H.K. Liu, S.X. Dou, Electrochemical deposition of porous $Co(OH)_2$ nanoflake films on stainless steel mesh for flexible supercapacitors, Journal of the Electrochemical Society 155 (2008) A926–A929.
[9] J. Fan, T. Wang, C. Yu, B. Tu, Z. Jiang, D. Zhao, Ordered nanostructured tin-based oxides/carbon composite as the negative-electrode material for lithium-ion batteries, Advanced Materials 16 (2004) 1432–1436.
[10] F.Y. Cheng, Z.L. Tao, J. Liang, J. Chen, Template-directed materials for rechargeable lithium-ion batteries, Chemistry of Materials 20 (2008) 667–681.
[11] Y. He, L. Huang, J.S. Cai, X.M. Zheng, S.G. Sun, Structure and electrochemical performance of nanostructured Fe_3O_4/carbon nanotube composites as anodes for lithium ion batteries, Electrochimica Acta 55 (2010) 1140–1144.
[12] M.Y. Cheng, B.J. Hwang, Mesoporous carbon-encapsulated NiO nanocomposite negative electrode materials for high-rate Li-ion battery, Journal of Power Sources 195 (2010) 4977–4983.
[13] J. Wang, G. Du, R. Zeng, B. Niu, Z. Chen, Z. Guo, S. Dou, Porous Co_3O_4 nanoplatelets by self-supported formation as electrode material for lithium-ion batteries, Electrochimica Acta 55 (2010) 4805–4811.
[14] Z.H. Li, T.P. Zhao, X.Y. Zhan, D.S. Gao, Q.Z. Xiao, G.T. Lei, High capacity three-dimensional ordered macroporous $CoFe_2O_4$ as anode material for lithium ion batteries, Electrochimica Acta 55 (2010) 4594–4598.
[15] Y. Lu, Y. Wang, Y. Zou, Z. Jiao, B. Zhao, Y. He, M. Wu, Macroporous Co_3O_4 platelets with excellent rate capability as anodes for lithium ion batteries, Electrochemistry Communications 12 (2010) 101–105.
[16] J.Y. Xiang, X.L. Wang, X.H. Xia, L. Zhang, Y. Zhou, S.J. Shi, J.P. Tu, Enhanced high rate properties of ordered porous Cu_2O film as anode for lithium ion batteries, Electrochimica Acta 55 (2010) 4921–4925.
[17] J. Jiang, J. Liu, R. Ding, X. Ji, Y. Hu, X. Li, A. Hu, F. Wu, Z. Zhu, X. Huang, Direct synthesis of CoO porous nanowire arrays on Ti substrate and their application as lithium-ion battery electrodes, Journal of Physical Chemistry C 114 (2010) 929–932.
[18] S. Wang, J. Zhang, C. Chen, Fe_3O_4 submicron spheroids as anode materials for lithium-ion batteries with stable and high electrochemical performance, Journal of Power Sources 195 (2010) 5379–5381.
[19] S.Q. Wang, J.Y. Zhang, C.H. Chen, Dandelion-like hollow microspheres of CuO as anode material for lithium-ion batteries, Scripta Materialia 57 (2007) 337–340.
[20] L. Yuan, Z.P. Guo, K. Konstantinov, P. Munroe, H.K. Liu, Spherical clusters of NiO nanoshafts for lithium-ion battery anodes, Electrochemical and Solid-State Letters 9 (2006) A524–A528.
[21] X. Guo, X. Lu, X. Fang, Y. Mao, Z. Wang, L. Chen, X. Xu, H. Yang, Y. Liu, Lithium storage in hollow spherical $ZnFe_2O_4$ as anode materials for lithium ion batteries, Electrochemistry Communications 12 (2010) 847–850.
[22] L. Liu, Y. Li, S. Yuan, M. Ge, M. Ren, C. Sun, Z. Zhou, Nanosheet-based NiO microspheres: controlled solvothermal synthesis and lithium storage performances, Journal of Physical Chemistry C 114 (2010) 251–255.
[23] H. Duan, J. Gnanaraj, X. Chen, B. Li, J. Liang, Fabrication and characterization of Fe_3O_4-based Cu nanostructured electrode for Li-ion battery, Journal of Power Sources 185 (2008) 512–518.
[24] J. Park, E. Kang, S.U. Son, H.M. Park, M.K. Lee, J. Kim, K.W. Kim, H.J. Noh, J.H. Park, C.J. Bae, J.G. Park, T. Hyeon, Monodisperse nanoparticles of Ni and NiO: synthesis, characterization, self-assembled superlattices, and catalytic applications in the Suzuki coupling reaction, Advanced Materials 17 (2005) 429–434.
[25] L. Li, E.A. Gibson, P. Qin, G. Boschloo, M. Gorlov, A. Hagfeldt, L.C. Sun, Double-layered NiO photocathodes for p-type DSSCs with record IPCE, Advanced Materials 22 (2010) 1759–1762.
[26] P. Qin, M. Linder, T. Brinck, G. Boschloo, A. Hagfeldt, L.C. Sun, High incident photon-to-current conversion efficiency of p-type dye-sensitized solar cells based on NiO and organic chromophores, Advanced Materials 21 (2009) 2993–2996.
[27] C.C. Yu, L.X. Zhang, J.L. Shi, J.J. Zhao, J.H. Gao, D.S. Yan, A simple template-free strategy to synthesize nanoporous manganese and nickel oxides with narrow pore size distribution, and their electrochemical properties, Advanced Functional Materials 18 (2008) 1544–1554.
[28] H. Pang, Q.Y. Lu, Y.C. Lia, F. Gao, Facile synthesis of nickel oxide nanotubes and their antibacterial, electrochemical and magnetic properties, Chemical Communications (2009) 7542–7544.
[29] S. Hosogai, H. Tsutsumi, Electrospun nickel oxide/polymer fibrous electrodes for electrochemical capacitors and effect of the heat treatment process on their performance, Journal of Power Sources 194 (2009) 1213–1217.
[30] J.Y. Lee, K. Liang, K.H. An, Y.H. Lee, Nickel oxide/carbon nanotubes nanocomposite for electrochemical capacitance, Synthetic Metals 150 (2005) 153–157.
[31] E. Hosono, S. Fujihara, I. Honma, H.S. Zhou, The high power and high energy densities Li ion storage device by nanocrystalline and mesoporous Ni/NiO covered structure, Electrochemistry Communications 8 (2006) 284–288.
[32] X.H. Huang, J.P. Tu, X.H. Xia, X.L. Wang, J.Y. Xiang, L. Zhang, Y. Zhou, Morphology effect on the electrochemical performance of NiO films as anodes for lithium ion batteries, Journal of Power Sources 188 (2009) 588–591.
[33] X.H. Huang, J.P. Tu, X.H. Xia, X.L. Wang, J.Y. Xiang, Nickel foam-supported porous NiO/polyaniline film as anode for lithium ion batteries, Electrochemistry Communications 10 (2008) 1288–1290.
[34] Y. Wang, Q.Z. Qin, A nanocrystalline NiO thin-film electrode prepared by pulsed laser ablation for Li-ion batteries, Journal of the Electrochemical Society 149 (2002) A873–A878.
[35] Y. Wang, Y.F. Zhang, H.R. Liu, S.J. Yu, Q.Z. Qin, Nanocrystalline NiO thin film anode with MgO coating for Li-ion batteries, Electrochimica Acta 48 (2003) 4253–4259.
[36] Y.N. Nuli, S.L. Zhao, Q.Z. Qin, Nanocrystalline tin oxides and nickel oxide film anodes for Li-ion batteries, Journal of Power Sources 114 (2003) 113–120.
[37] K.F. Chiu, C.Y. Chang, C.M. Lin, The electrochemical performance of bias-sputter-deposited nanocrystalline nickel oxide thin films toward lithium, Journal of Electrochemical Society 152 (2005) A1188–A1192.
[38] H.B. Wang, Q.M. Pan, X.P. Wang, G.P. Yin, J.W. Zhao, Improving electrochemical performance of NiO films by electrodeposition on foam nickel substrates, Journal of Applied Electrochemistry 39 (2009) 1597–1602.
[39] Q.M. Pan, J. Liu, Facile fabrication of porous NiO films for lithium-ion batteries with high reversibility and rate capability, Journal of Solid State Electrochemistry 13 (2009) 1591–1597.
[40] A.A. Al-Ghamdi, W.E. Mahmoud, S.J. Yaghmour, F.M. Al-Marzouki, Structure and optical properties of nanocrystalline NiO thin film synthesized by sol–gel spin-coating method, Journal of Alloys and Compounds 486 (2009) 9–13.
[41] X.H. Huang, J.P. Tu, C.Q. Zhang, X.T. Chen, Y.F. Yuan, H.M. Wu, Spherical NiO–C composite for anode material of lithium ion batteries, Electrochimica Acta 52 (2007) 4177–4181.

[42] X.H. Huang, J.P. Tu, C.Q. Zhang, J.Y. Xiang, Net-structured NiO–C nanocomposite as Li-intercalation electrode material, Electrochemistry Communications 9 (2007) 1180–1184.
[43] F. Davar, Z. Fereshteh, M. Salavati-Niasari, Nanoparticles Ni and NiO: synthesis, characterization and magnetic properties, Journal of Alloys and Compounds 476 (2009) 797–801.
[44] M. Salavati-Niasari, F. Davar, Z. Fereshteh, Synthesis of nickel and nickel oxide nanoparticles via heat-treatment of simple octanoate precursor, Journal of Alloys and Compounds 494 (2010) 410–414.
[45] A.C. Sonavane, A.I. Inamdar, P.S. Shinde, H.P. Deshmukh, R.S. Patil, P.S. Patil, Efficient electrochromic nickel oxide thin films by electrodeposition, Journal of Alloys and Compounds 489 (2010) 667–673.
[46] X.H. Huang, J.P. Tu, Z.Y. Zeng, J.Y. Xiang, X.B. Zhao, Nickel foam-supported porous NiO/Ag film electrode for lithium-ion batteries, Journal of Electrochemical Society 155 (2008) A438–A441.
[47] X.H. Huang, J.P. Tu, X.H. Xia, X.L. Wang, J.Y. Xiang, L. Zhang, Porous NiO/poly(3,4-ethylenedioxythiophene) films as anode materials for lithium ion batteries, Journal of Power Sources 195 (2010) 1207–1210.
[48] H.R. Liu, W.M. Zheng, X. Yan, B.X. Feng, Studies on electrochromic properties of nickel oxide thin films prepared by reactive sputtering, Journal of Alloys and Compounds 462 (2008) 356–361.
[49] T.L. Lai, Y.Y. Shu, G.L. Huang, C.C. Lee, C.B. Wang, Microwave-assisted and liquid oxidation combination techniques for the preparation of nickel oxide nanoparticles, Journal of Alloys and Compounds 450 (2008) 318–322.
[50] H.L. Wang, H.S. Casalongue, Y.Y. Liang, H.J. Dai, $Ni(OH)_2$ nanoplates grown on graphene as advanced electrochemical pseudocapacitor materials, Journal of the American Chemical Society 132 (2010) 7472–7477.
[51] D. Aurbach, Review of selected electrode–solution interactions which determine the performance of Li and Li ion batteries, Journal of Power Sources 89 (2000) 206–218.
[52] P. Poizot, S. Laruelle, S. Grugeon, L. Dupont, J.M. Tarascon, Searching for new anode materials for the Li-ion technology: time to deviate from the usual path, Journal of Power Sources 97–98 (2001) 235–239.
[53] H. Qiao, N. Wu, F. Huang, Y. Cai, Q. Wei, Solvothermal synthesis of NiO/C hybrid microspheres as Li-intercalation electrode material, Materials Letters 64 (2010) 1022–1024.
[54] S.A. Needham, G.X. Wang, H.K. Liu, Synthesis of NiO nanotubes for use as negative electrodes in lithium ion batteries, Journal of Power Sources 159 (2006) 254–257.
[55] X. Wang, X. Li, X. Sun, F. Li, Q. Liu, Q. Wangab, D. He, Nanostructured NiO electrode for high rate Li-ion batteries, Journal of Materials Chemistry 21 (2011) 3571–3573.
[56] H.W. Lee, P. Muralidharan, R. Ruffo, C.M. Mari, Y. Cui, D.K. Kim, Ultrathin spinel $LiMn_2O_4$ nanowires as high power cathode materials for Li-ion batteries, Nano Letters 10 (2010) 3852–3856.
[57] C. Wang, D. Wang, Q. Wang, H. Chen, Fabrication and lithium storage performance of three-dimensional porous NiO as anode for lithium-ion battery, Journal of Power Sources 195 (2010) 7432–7437.
[58] N. Sharma, J. Plevert, G.V. Subba Rao, B.V.R. Chowdari, T.J. White, Tin oxides with hollandite structure as anodes for lithium ion batteries, Chemistry of Materials 17 (2005) 4700–4710.
[59] M.S. Park, Y.M. Kang, G.X. Wang, S.X. Dou, H.K. Liu, The effect of morphological modification on the electrochemical properties of SnO_2 nanomaterials, Advanced Functional Materials 18 (2008) 455–461.
[60] S. Yang, H. Song, X. Chen, Electrochemical performance of expanded mesocarbon microbeads as anode material for lithium-ion batteries, Electrochemistry Communications 8 (2006) 137–142.
[61] Y.J. Mai, J.P. Tu, X.H. Xia, C.D. Gu, X.L. Wang, Co-doped NiO nanoflake arrays toward superior anode materials for lithium ion batteries, Journal of Power Sources 196 (2011) 6388–6393.
[62] I. Belharouak, G.M. Koenig Jr., K. Amine, Electrochemistry and safety of $Li_4Ti_5O_{12}$ and graphite anodes paired with $LiMn_2O_4$ for hybrid electric vehicle Li-ion battery applications, Journal of Power Sources 196 (2011) 10344–10350.